

Climate over South America in regional model simulations

S. Wagner et al.

Climatic changes between 20th century and pre-industrial times over South America in regional model simulations

S. Wagner¹, I. Fast², and F. Kaspar³

¹Helmholtz-Zentrum Geesthacht, Geesthacht, Germany

²German Climate Computing Center – DKRZ, Hamburg, Germany

³Deutscher Wetterdienst – DWD, Offenbach, Germany

Received: 1 September 2011 – Accepted: 13 September 2011

– Published: 22 September 2011

Correspondence to: S. Wagner (sebastian.wagner@hzg.de)

Published by Copernicus Publications on behalf of the European Geosciences Union.

Title Page

Abstract

Introduction

Conclusions

References

Tables

Figures

⏪

⏩

◀

▶

Back

Close

Full Screen / Esc

Printer-friendly Version

Interactive Discussion



Abstract

Two simulations with a regional climate model are analyzed for climatic changes between the late 20th century and a pre-industrial period over central and southern South America. The model simulations have been forced with large-scale boundary data from the global simulation performed with a coupled atmosphere-ocean general circulation model. The regional simulations have been carried out on a $0.44^\circ \times 0.44^\circ$ grid (approx. 50 km \times 50 km horizontal resolution). The differences in the external forcings are related to a changed greenhouse gas content of the atmosphere, being higher in the present-day simulation.

For validation purposes the climate model is analyzed using a five year long simulation between 1993 and 1997 forced with re-analysis data. The climate model reproduces the main climatic features reasonably well, especially when comparing model output co-located with observational station data. However, the comparison between observed and simulated climate is hampered by the sparse meteorological station network in South America.

The present-day simulation is compared with the pre-industrial simulation for atmospheric fields of near-surface temperatures, precipitation, sea level pressure and zonal wind. Higher temperatures in the present-day simulation are evident over entire South America, mostly pronounced over the southern region of the Andes Mountains and the Parana basin. During southern winter the higher temperatures prevail over the entire continent, with largest differences over the central Andes Mountains and the Amazonian basin.

Precipitation differences show a more heterogeneous pattern, especially over tropical regions. This might be explained by changes in convective processes acting on small scales. During southern summer wetter conditions are evident over the Amazonian and Parana basin in the present-day simulation. Precipitation increases are evident over Patagonia together with decreases to the north along the western slope of the Andes Mountains. During southern winter also a dipole pattern along the Andes

Climate over South America in regional model simulations

S. Wagner et al.

Title Page

Abstract

Introduction

Conclusions

References

Tables

Figures



Back

Close

Full Screen / Esc

Printer-friendly Version

Interactive Discussion



Mountains with wetter conditions over the southern parts and drier conditions over the central parts is evident. An interesting feature relates to precipitation changes with changing sign within a few 10th of kilometers along the southern parts of the Andes mountain chain. This pattern can be explained by changes in large-scale circulation related to latitudinal changes of the extratropical southern hemispheric westerlies.

1 Introduction

The climate of South America is influenced by the interplay of different large-scale atmospheric and oceanic phenomena and topographic features of the continent. In the central and northern parts this relates to convective processes linked to the seasonal movements of the Inner Tropical Convergence Zone (ITCZ). The inter-annual variability in the position of the ITCZ is controlled by the state of the Pacific Ocean that is largely influenced by the El-Niño-Southern Oscillation (ENSO) phenomenon in this region. In the central western parts of South America the Pacific anticyclone and the cold Humboldt Current influence the coastal region and lead to the formation of the Atacama Desert.

An important climatic characteristic in the extra-tropical parts of South America are the westerly winds. These are caused by the planetary frontal zone with the deepest gradients between warm subtropical air in low latitudes and cold polar and subpolar air in high latitudes. In general, the westerlies show different latitudinal positions at different tropospheric levels. For instance, during southern winter the jet streams in the upper troposphere are located over the subtropics, whereas the near-surface westerlies are located further to the south over the mid-latitudes (cf. also Fig. 11, Wagner et al., 2007).

From a seasonal point of view the westerly wind belt moves in north-south direction, depending on the position of the ITCZ which itself is controlled by the position of the sun. Therefore the westerlies show a more northward location during southern winter and a more southerly position during southern summer. An interesting phenomenon is the fact that the westerlies show their highest wind speed during southern summer

Climate over South America in regional model simulations

S. Wagner et al.

Title Page

Abstract

Introduction

Conclusions

References

Tables

Figures



Back

Close

Full Screen / Esc

Printer-friendly Version

Interactive Discussion



Climate over South America in regional model simulations

S. Wagner et al.

Title Page

Abstract

Introduction

Conclusions

References

Tables

Figures

◀

▶

◀

▶

Back

Close

Full Screen / Esc

Printer-friendly Version

Interactive Discussion



(cf. Garreaud et al., 2009, Fig. 3a). This is because the meridional temperature gradients between the subtropical and subpolar regions are stronger during austral summer than during austral winter. These stronger gradients are caused by the very low temperatures over Antarctica also during summer and the increased temperatures over the subtropical latitudes. The gradients lead to strong geostrophic winds in the upper troposphere, extending also into the lower levels. The climatic effect of the westerlies, especially over the southern parts of South America, relates to the advection of mild and moist air masses from the Pacific Ocean onto the western slopes of the Andes Mountains causing high precipitation amounts in these areas. On the eastern parts of the Mountain chain the descending air masses lead to dryness evoking the formation of the Patagonian steppe (Garreaud et al., 2009).

Compared to the Northern Hemisphere the mean westerly wind speed is higher in the Southern Hemisphere. Therefore also the duration of blocking episodes is reduced and meridional circulation types are underrepresented compared to the Northern Hemisphere (cf. Table 6 Wiedenmann et al., 2002). Specifically for South America the Andes Mountains play an important role in generating disturbances in the westerly flow in terms of stream-flow deflections. In this context, deflections to the North lead to cold Antarctic outbreaks over the eastern side of the Andes Mountains (cf. Garreaud, 2000; Seluchi et al., 2006). Southward deflections of the jet stream in this regions lead to the intrusion of warm subtropical air masses leading to precipitation in the Pampa region. Together with the prevailing Chaco-low, these northerly winds often occur during austral summer, channelling the air motion between the eastern parts of the Andes Mountains and the Brazilian Plateau (Seluchi et al., 2006).

The present model study was carried out in a framework with different simulations covering different periods of the Holocene climate. One intention among others was to test hypotheses that are based on empirical evidence by means of regional climate model simulations. In the following a brief overview about empirical studies and their results will therefore be provided. In the context of empirical paleoclimate reconstructions a number of studies have been carried out addressing the influence of the large-scale

atmospheric circulation on southern South America. From the empirical side Lamy et al. (2010) investigate changes in westerly winds at the extratropical western margin of the Andes Mountains based on marine sediments and pollen records. The records indicate an anti-phasing between the center of the westerlies and their northern margin.

5 Accordingly, during the early Holocene the wind speed in the latitude of maximum westerly wind speed was more pronounced, whereas the northern margin was weak. In the course of the Holocene this pattern reversed. The authors suggest that the variability in the westerlies is largely determined by the sea surface temperatures (SSTs) in the eastern South Pacific. For the more northern regions, to the eastern side of the Andes Mountains, Markgraf et al. (2003) analyze lacustrine sediments of Lago Cardiel. The authors link changes in proxy records with changes in the position and intensity of westerly winds, more specifically the storm tracks. Based on qualitative upscaling models of proxy information authors suggest that the storm tracks were more zonal in the early Holocene north of 50° S. The authors also hypothesize that this led to more Antarctic cold fronts advecting moisture from the Atlantic Ocean into southeastern Patagonia. For the late Holocene the storm tracks were more meridional in character resulting in less and more variable precipitation. For south-eastern Patagonia Mayr et al. (2005) analyzed a multi-proxy data contained in a lake sediment core of Laguna Azul to reconstruct environmental and climatic conditions of the last millennium. Changes in carbon isotopes during the period of the Little Ice Age (LIA) are interpreted as cooler conditions in conjunction with increased lake levels. Other perturbations, occurring at the beginning of the 19th century could however be linked to anthropogenic influence in this region in the context of the European settlement. The latter point emphasizes the need for a thorough analysis of proxy data and interpretation in regions where the human influence increased in the course of the recent centuries. The human impact in southeastern Patagonia is also addressed in the study of Ariztegui (2009) pointing to the link between an increase in human occupation with decreases in lake levels in the Lago Cardiel basin.

Climate over South America in regional model simulations

S. Wagner et al.

Title Page

Abstract

Introduction

Conclusions

References

Tables

Figures



Back

Close

Full Screen / Esc

Printer-friendly Version

Interactive Discussion



in the 20th century in southern Patagonia during southern summer and a decrease in precipitation over most regions of southern South America during southern winter.

From a modeling point of view in the context of General Circulation Model (GCM) simulations, Rojas et al. (2009) investigate changes in the extratropical southern hemispheric westerlies for different time slices in the past 21 000 yr in selected simulations that were carried out in the framework of the 2nd phase of the Paleoclimate Intercomparison Project (PMIP II). The study demonstrates the virtue of a comparison among different GCMs for discriminating climate- and model specific responses on changes in external forcing parameters respectively. For example, the models used in the study do not show a uniform response to changes in the external forcing conditions. According to Fig. 9 of Rojas et al. (2009), over southern South America some models show an increase in westerly winds whereas others show a decrease related to differences between Last Glacial Maximum (LGM) and pre-industrial (PI) conditions. Although the study analyses differences between LGM and PI conditions that were presumably larger in terms of changes in external forcing parameters than differences in between present-day and pre-industrial times, this demonstrates the high degree of disagreement between different GCMs under the same external forcing conditions. Another study carried out by de Melo and Marengo (2008) also analyze the influence of external orbital parameters on the climate of South America during the mid-Holocene. Results indicate a decrease of precipitation over southeastern South America compared to pre-industrial times. Also, the simulation shows a decrease in temperatures over the eastern parts of the Andes Mountains, caused by more frequent Antarctic cold outbreaks during southern summer and autumn. Wagner et al. (2007) carried out a study analyzing changes in westerly winds over southern South America and its influence on precipitation changes over southeastern Patagonia. Based on a downscaling of the large-scale circulation of the GCM authors conclude that precipitation changes in eastern Patagonia are caused by blocking of the westerly winds in conjunction with an eastward advection of humid air from the southwestern Atlantic. A comparative study of Varma et al. (2011) based on different GCM simulations analyses transient changes

Climate over South America in regional model simulations

S. Wagner et al.

Title Page

Abstract

Introduction

Conclusions

References

Tables

Figures



Back

Close

Full Screen / Esc

Printer-friendly Version

Interactive Discussion



on the westerlies in the course of the Holocene. The authors suggest a prominent influence of changes in solar activity controlling the position of the westerlies with periods of higher solar activity being linked to a more poleward position of the westerlies, whereas periods of reduced solar activity may cause a more equatorward position.

5 Early studies using regional climate models over South America have been undertaken for instance by Rojas and Seth (2003) and Misra et al. (2003). The latter carry out a dynamical downscaling for a seasonal GCM simulation for southern summer with a horizontal resolution of 80 km using pre-scribed SSTs. The authors point to the improvements for vertical and horizontally resolved atmospheric circulation character-
10 istics and precipitation in the RCM as well as a reduction of model biases evident in the GCM. Rojas and Seth (2003) undertake sensitivity studies with a RCM with a nested modeling system over South America to investigate the effects of SSTs, vegetation and soil moisture on simulated climate as well as and the sensitivity of the RCM to domain size. For the SST boundary forcing, for example, the RCM shows a pronounced
15 response resulting in rainfall differences between a wet and dry year, indicating the important influence of the external boundary forcing on the interior of the domain, related to changes in moisture transport and advection.

More recent regional climate model studies for the region of central and southern South America have been undertaken by Solman et al. (2008) and Nunez et al. (2008).
20 The authors carried out climate simulations with the regional climate model MM5 forced with the global model HadAM3H for present-day and a future period. The study of Solman et al. (2008) encompasses comparisons between the HadAM3H+MM5 simulation and meteorological observations in the period 1981–1990. Authors conclude that the HadAM3H+MM5 model is able to realistically reproduce climatic patterns of important meteorological variables (temperature, precipitation, sea level pressure) and their
25 short- and long term variability over South America. However, for some regions distinct differences between the regional climate model simulation and the observational data sets are evident. The study of Nunez at al. (2008) investigates two greenhouse gas emission scenarios (SRES A2 and B2) for the period 2081–2090. Model results

Climate over South America in regional model simulations

S. Wagner et al.

Title Page

Abstract

Introduction

Conclusions

References

Tables

Figures



Back

Close

Full Screen / Esc

Printer-friendly Version

Interactive Discussion



5 indicate seasonally dependent changes with increased precipitation during southern summer and autumn and reduced precipitation during winter and spring compared to the 1981–1990 period. The corresponding circulation changes point to a southward extension of the subtropical Pacific and Atlantic high pressure cell in comparison with the reference period 1981–1990. The study by Silvestri et al. (2009) analyses a hind-cast with re-analysis data for the whole South American continent downscaled with the RCM REMO. The authors state that the RCM considerably improves atmospheric circulation related to the summer monsoon circulation, the Bolivian High and the related subtropical jet. Also the precipitation cycle is represented reasonably well, albeit with overestimations in tropical and subtropical regions. For temperature the bias is below 1.5 K. The authors conclude that the REMO RCM improves the global reanalysis data specifically for temperature in the tropical regions during the warm season and for precipitation in the subtropics and extratropical regions.

10 For the more distant geological past, Poulsen et al. (2010) and Insel et al. (2010) investigate the influence of the uplift of the Andes Mountains on the climate of South America. Insel et al. (2010) carry out studies with a RCM simulating different altitude stages of the Andes Mountains. The simulations indicate that the formation of the Andes Mountains was crucial for the formation of the South American low level jet and the blocking of the westerly winds. From a hydrological perspective this implied changes in the moisture transport between the Amazonian basin and the central Andes. Poulsen et al. (2010) analyze the onset of convective rainfall in the late Miocene by means of regional climate models and compare results to proxy data information based on $\delta^{18}\text{O}$. Their results also indicate that the uplift of the Andes Mountains was crucial for high convective summer precipitation rates on the eastern side of the Andean Plateau.

25 The studies introduced above show that RCMs show improvements regarding regional-to-local scale climatic information, especially related to hydrological processes. This is not only true for present-day or future climatic analysis but is also of specific interest from the paleo perspective. Therefore, it can be supposed that the integration of a RCM forced by the output of a GCM may help to better mimic

Climate over South America in regional model simulations

S. Wagner et al.

Title Page

Abstract

Introduction

Conclusions

References

Tables

Figures



Back

Close

Full Screen / Esc

Printer-friendly Version

Interactive Discussion



hydrological processes on regional-to-local scales, serving as important basis in the context of model-data comparisons and for the performance of climate impact studies.

As already mentioned above, a technical point of specific interest in regional climate modeling relates to the influence of the driving GCM. Although the dynamical core and physical parametrizations of the regional climate model in general differ from the one of the driving, global climate model, the information entering through its boundaries will have a profound influence on the basic structure of the interior (see also the discussion in Gomez-Navarro et al., 2011). This fact is important because it implies that the large-scale circulation is largely determined by the state of the driving model. Given that the models are driven with the same external boundary forcings as for instance realized within coupled model-intercomparison projects in the context of CMIP (Meehl et al., 2000), PMIP I (PMIP, 2000) and PMIP II (Braconnot, 2007), the mean state and variability may vary between different GCMs. An important point is also that some boundary conditions may not well be known, especially when oceanic processes acting on longer temporal scales come into play (cf. Valdes, 2000). Therefore it is important to note that results of regional climate models present only one out of many different possible realizations. For example, the PRUDENCE project investigated this issue for the European realm. Results indicate that different combinations of global and regional climate models may considerably differ concerning the climatic response for both, the sign and magnitude of changes between a future climate simulation and a control period (cf. Frei et al., 2005). This point is of specific relevance because this study only presents results for a single GCM+RCM experiment setup.

The paper is structured as follows: In the next paragraph the global and regional climate models are introduced including the experimental setup. The following section includes the validation of the climate models for selected atmospheric variables in representing the annual cycle for single stations and spatially resolved fields. Section 3 contains the discussion of climatic differences between the simulations carried out for present-day and pre-industrial times. In Sect. 4 changes in westerly winds are discussed as driving mechanism for hydrological changes. Section 5 includes the

Climate over South America in regional model simulations

S. Wagner et al.

Title Page

Abstract

Introduction

Conclusions

References

Tables

Figures



Back

Close

Full Screen / Esc

Printer-friendly Version

Interactive Discussion



summary and conclusions of the study. The study is closed with an outlook contained within Sect. 6.

2 Climate models and experimental setup

The global model used for all experiments is the coupled atmosphere ocean general circulation model ECHO-G (Legutke and Voss, 1999; Min et al., 2005). The model consists of the atmospheric model ECHAM4 (Roeckner et al., 1996) coupled to the oceanic model HOPE-G (Wolff et al., 1997). The atmospheric component is a spectral model with a horizontal resolution of T30 (approx. 3.75° lat \times 3.75° lon) and 19 vertical levels. The ocean model HOPE-G has 20 vertical levels and an effective horizontal resolution of approximately 2.8° lat \times 2.8° lon with a gradual meridional refinement (reaching 0.5°) towards the equator in order to better represent ENSO-related processes.

For the regional simulations the climate model CCLM, the climate version of the non-hydrostatic limited-area operational weather prediction model of the Consortium on Small scale Modeling (COSMO), has been used (Boehm et al., 2003; Rockel et al., 2008). For all simulations the model version CCLM 4.2 has been used. The model is setup on rotated spherical coordinates with a resolution of $0.44^\circ \times 0.44^\circ$, corresponding to a horizontal grid point distance of approx. $50 \text{ km} \times 50 \text{ km}$. The geographical domain consists of 128×103 grid points in the latitudinal and longitudinal direction, respectively. The center of the domain is located at 62.5° W ; 40° S . For the analysis of model results the fields have been interpolated onto a regular geographical grid with a horizontal resolution of $50 \text{ km} \times 50 \text{ km}$, also for better comparison with observationally based and gridded data sets.

The regional simulations have been forced at the lateral boundaries with six hourly data from the ECHO-G model. Each time slice experiment has been carried out for 35 yr. For analysis the first five years have been neglected in order to let the interior of the regional model fully adapt to changes in external conditions. The CO_2 concentrations have been set to 330 ppm for the present-day (PD) simulation and to 280 ppm

Climate over South America in regional model simulations

S. Wagner et al.

Title Page

Abstract

Introduction

Conclusions

References

Tables

Figures



Back

Close

Full Screen / Esc

Printer-friendly Version

Interactive Discussion



for the pre-industrial (PI) simulation in the regional model. The value of 330 ppm corresponds approximately to the greenhouse gas concentrations in the mid 1970s in the ECHO-G simulation and is set as default value by the German Weather Service within CCLM. All simulations have been carried out with the same surface boundary forcing field, i.e. vegetation and other surface and soil properties.

Figure 1 shows a comparison between topography in the driving ECHO-G GCM and the regional climate model CCLM. In the regional climate model CCLM the representation of regional topographic features is considerably improved. For example, the Andes Mountains can only hardly be figured out in the ECHO-G model. Also their absolute height is very low compared to real world. The better representation of the complex topography and also of the absolute heights is a pre-requisite to more realistically simulate regional climatic processes.

3 Validation of the regional model with observational data sets

Model validation is a crucial point in regional climate modeling, because it is not a priori guaranteed that the increased resolution of the regional model compared to the global model produces better results. This is especially true for hydrological variables like precipitation. For example, simulations already carried out over South America by Solman et al. (2008) with the regional climate model MM5 forced with the global GCM HadAM3H show distinct differences compared to quasi-observational data in selected regions over South America.

For the validation a five year (1993–1997) long CCLM simulation forced with data from the European Center for Medium Weather Forecast (ECMWF) 40 Year Re-analysis Project (ERA-40) has been carried out. In the following section a comparison between different observational data sets for selected locations is carried out. The locations have been selected based on the different regions introduced by Solman et al. (2008). For better comparative purposes however not the areal average of the region has been used. Instead, a grid point co-located with a meteorological station

Climate over South America in regional model simulations

S. Wagner et al.

Title Page

Abstract

Introduction

Conclusions

References

Tables

Figures



Back

Close

Full Screen / Esc

Printer-friendly Version

Interactive Discussion



within the respective region has been selected from the regional climate model simulation and then compared with a grid point out of the observational data set. The rationale is that due to the high spatial variability for precipitation, the comparison of areal averages might be flawed by the sparseness of observational data. In a second section a spatially resolved analysis will be carried out for central and southern South America.

Observational gridded data sets used for comparison are the data products of the Climate Research Unit (CRU, Mitchell and Jones, 2005) for temperature, the “Global Precipitation Climatology Center (GPCC) Climatology Version 2010” for mean monthly precipitation, the “GPCC Full Data Reanalysis Version 5” time series of monthly means (Rudolf et al., 2010), and the National Center for Environmental Prediction and National Center for Atmospheric Research (NCEP/NCAR) re-analysis (Kistler et al., 2001) for sea level pressure.

3.1 Validation based on single grid points

Figure 2a and b show the annual temperature and precipitation cycle for grid points co-located with sites where observational data are available (cf. Table 1). In Fig. 1 the locations have been plotted from North to South taking into account the different latitudes of the station.

The annual cycle of temperature is reproduced for all locations reasonably well, except for the location of Antofagasta (Central Andes, CA) where it is shifted with respect to the CRU data set. The absolute temperature level is however different for most locations. Most locations show absolute values that are too low with respect to the CRU data set. Only locations in the central and southern western Andes regions (Santiago de Chile, Subtropical Andes, SUA) and Puerto Montt (Southern Andes, SA) show modeled temperatures that are too high compared to the CRU data set.

For precipitation the pattern is more complex for the different locations (Fig. 2b). For the northwestern location Antofagasta (CA) the annual precipitation cycle is reproduced very well. For the northern location of Porto Alegre (Southern Brazil, SB)

Climate over South America in regional model simulations

S. Wagner et al.

Title Page

Abstract

Introduction

Conclusions

References

Tables

Figures



Back

Close

Full Screen / Esc

Printer-friendly Version

Interactive Discussion



the absolute values are mostly underestimated by the ERA40+CCLM simulation. The more southern locations show higher agreement with observations. For Santiago de Chile (SUA) the precipitation maximum is however over-estimated, whereas for Puerto Montt (SA) the simulation is very close to the GPCC data set. The station representing Rio Gallegos in Argentinean Patagonia (AP) shows simulated values that are too high.

3.2 Validation based on spatially gridded fields

As already mentioned in the last paragraph, a caveat in validating model results over South America originates from the scarcity of meteorological observations. Another very crucial point relates to the high complexity of the terrain, especially in its western part occupied by the Andes Mountains. From the European Alps it is known that precipitation amounts can vary by a factor of two between stations located in the valley of an alpine chain compared to a high elevated station on a mountain top. This point is very important because in southern South America no summit stations are available for the Andes Mountains. Neglecting this effect would potentially lead to a false interpretation of results obtained by the climate model simulation. This point has also been highlighted by Solman et al. (2008), stating that differences in mountainous regions between their MM5 simulations and other gridded reanalysis data products can be larger than 80 %. Silvestri et al. (2009) also state that the differences between station heights and the mean height of model grid boxes complicate the comparison between observations and results from the regional climate model.

Figures 3 to 6 contain results for the validation for spatially resolved fields of the different simulations used in the study. Besides the ERA40+CCLM simulation for the period 1993–1997 also results for the CCLM simulation and the driving ECHO-G simulation for the late 20th century are given. For the latter 31 yr averages for the period 1960–1990 for the observational data sets have been used together with 31 yr of the regional (ECHO-G+CCLM) and global (ECHO-G) climate model as a basis for comparison.

Climate over South America in regional model simulations

S. Wagner et al.

Title Page

Abstract

Introduction

Conclusions

References

Tables

Figures



Back

Close

Full Screen / Esc

Printer-friendly Version

Interactive Discussion



Climate over South America in regional model simulations

S. Wagner et al.

Title Page

Abstract

Introduction

Conclusions

References

Tables

Figures



Back

Close

Full Screen / Esc

Printer-friendly Version

Interactive Discussion



The mean temperature fields of the ERA40+CCLM simulation for the period 1993–1997 are displayed in the left column of Fig. 3. The simulation reasonably well reproduces the basic climatological features of temperature field for central and southern South America. For example, the Andes Mountains in the South and the Altiplano region to the North show considerably lower temperatures in contrast to the lower altitude parts to the east related to the Amazonian and Parana basin. The model even discriminates the coastal parts at the western coast of South America showing higher temperatures. Lower temperatures during southern winter in the Andes Mountain chain including the Altiplano are also well captured. Patagonia is characterized by very low temperatures. Also the subtropical regions show distinct cooler temperatures compared to the summer situation. In the central parts of South America temperatures remain high due to the equatorward position of these regions.

Differences between the ERA40+CCLM simulation and CRU temperatures (2nd column) show mainly a cold bias over most regions, except for an overestimation along the coast of western South America. This pattern is similar throughout the year. The pattern is also consistent with results obtained in the single grid point analysis. Differences between the ECHO-G+CCLM simulation (3rd column) as well as the driving ECHO-G simulation (4th column) deviate from the ERA40+CCLM data showing positive temperature biases in most regions. These are mostly pronounced over the Andes Mountains in the central and Northern parts and the Parana basin in the ECHO-G model. The temperature bias in the ECHO-G model over the Andes Mountains and also to the east is however considerably reduced in the ECHO-G+CCLM simulation due to the higher spatially resolved topography in the regional simulation.

The precipitation fields are displayed in Fig. 4. The left column shows the mean climatic conditions for the ERA40+CCLM simulation. During southern summer high precipitation sums are evident over the central and subtropical parts. This is due to the southward position of the ITCZ and the accompanying establishment of continental low pressure systems, generating convective summer precipitation. Also the dry region of the Atacama Desert extending south into the eastern parts of the Pampas is

reflected in the model simulation. In the southernmost parts the Andes mountain chain is reflected by high precipitation along the western parts of the Mountains. During southern winter precipitation is reduced over the central parts. Also the central parts of the Andes Mountains and the Altiplano receive less precipitation due to the northward displacement of the ITCZ. Over the eastern highland of south-east Brazil precipitation is increased compared to the surrounding areas. Along the western side of the Andes Mountains the region of higher precipitation is extended towards lower latitudes.

Precipitation differences between the ERA40+CCLM simulation and the GPCP data set show an underestimation over southeastern Brazil by the regional model, mostly pronounced during southern summer. Another region showing prominent differences is located in the southern parts of the Andes Mountains. Here the model simulates precipitation amounts that are higher compared to the GPCP data. It should be noted that in this region comparatively few meteorological observations are available and therefore results might be influenced by the sparseness of observational data. For example, the map presented in the study of Villa-Martinez and Moreno (2007) shows yearly precipitation sums up to 7000 mm along the southern Andes Mountains. Precipitation differences of the ECHO-G+CCLM and ECHO-G simulation are more similar to the ERA40+CCLM simulation compared to temperature difference patterns. This relates to the over-estimation of precipitation along the Andes Mountains in the ECHO-G+CCLM simulation and the underestimation in southeastern Brazil and the Parana region. According to Vera et al. (2006) this pattern is already evident in the global model and is caused by too high sea level pressure, preventing the generation of precipitation in this region (cf. also Fig. 5). The ECHO-G model does however not show the confinement of the positive precipitation bias to the western slopes of the Andes Mountains due to the underrepresentation of the local topographic features.

The mean sea level pressure fields of the ERA40+CCLM simulation are displayed in the left column of Fig. 5. In southern summer and winter the isobars over southern South America run east-west indicating a prominent westerly flow. Off the coast of South America the influence of the southeastern Pacific anticyclone is evident. Over

Climate over South America in regional model simulations

S. Wagner et al.

Title Page

Abstract

Introduction

Conclusions

References

Tables

Figures



Back

Close

Full Screen / Esc

Printer-friendly Version

Interactive Discussion



the tropical parts low pressure is characteristic for southern summer. During southern winter the pressure over the Parana basin and south-eastern Brazil is increased, regions to the South still show a prominent pressure gradient, resulting in a pronounced westerly circulation.

5 Pressure differences between the ERA40+CCLM simulations and the NCEP/NCAR reanalysis show a very similar pattern in all seasons. This relates to the already mentioned overestimation of the pressure over south-east Brazil and Patagonia. The differences for the ECHO-G+CCLM are similar to results obtained for the ERA40+CCLM simulation with pressure over eastern South America that is too high in all seasons.
10 This positive pressure bias is also reported by Solman et al. (2008) for the MM5 model. The positive pressure bias over south-eastern Brazil results in the already mentioned negative precipitation bias over this region. A mechanism possibly influencing this bias might be an underestimation of Antarctic cold outbreaks generating so called Chaco lows. Although these low pressure systems are not very long lasting they account for
15 a huge amount of precipitation generated in northeastern Argentina (cf. Salio et al., 2002).

Moreover, the ECHO-G+CCLM and the driving ECHO-G simulation show pronounced negative pressure differences in the southwestern parts, especially during southern winter. In conjunction with the positive pressure bias over the subtropical
20 parts this leads to an increased westerly flow over southern South America compared to the reanalysis data, explaining part of the overestimation of precipitation along the western slope of Andes Mountains. Another difference of the ECHO-G model relates to the underestimation of pressure over Altiplano, mostly pronounced during southern summer that is again caused by the lack of a detailed topography in the GCM.

Climate over South America in regional model simulations

S. Wagner et al.

Title Page

Abstract

Introduction

Conclusions

References

Tables

Figures



Back

Close

Full Screen / Esc

Printer-friendly Version

Interactive Discussion



4 Differences between the present-day and the pre-industrial climate

4.1 Near-surface temperatures, precipitation and sea level pressure

In the following differences between the present-day period representing conditions of the second half of the 20th century and the pre-industrial period representing conditions of 1750 AD for selected atmospheric variables will be presented. These variables include temperature, precipitation, sea level pressure as well as zonal winds at 850 hPa, 500 hPa, and 200 hPa. To test the significance of the differences a Student's t-test has been applied. In the Figures the 5% level of significance (2-sided test) is included in the maps. As already mentioned above, the difference between the present-day (PD) and pre-industrial (PI) simulation relates to the content of atmospheric greenhouse gases in terms of CO₂ (i.e. 330 ppm and 280 ppm, respectively). Therefore differences between the PD and PI simulation are caused by the increase in greenhouse gases.

Figure 6 shows the differences between the different variables for southern summer (December–February) and winter (June–August) and the annual mean, respectively. The temperature patterns (cf. left panel of Fig. 6) mostly show higher temperatures during PD than PI over central and southern South America. Largest temperature differences are evident over the Andes Mountains extending into the Pampas during southern summer. During southern winter a similar pattern is evident albeit with highest temperatures during PD extending further northwards over the Andes Mountains and into the Amazonian basin. On the annual average entire South America shows temperatures during PD that are increased in the order of 1.5 K, over the Andes Mountains by 2.1 K, compared to PI.

Precipitation differences (cf. middle panel of Fig. 6) are more heterogeneous compared to near-surface temperatures for both, magnitude and spatial variability. For example, wetter conditions during PD are evident over most of the Southern Ocean and the southern tip of South America. Over central South America the pattern is more complex. This might be related to the different type of precipitation dynamics in these

Climate over South America in regional model simulations

S. Wagner et al.

Title Page

Abstract

Introduction

Conclusions

References

Tables

Figures



Back

Close

Full Screen / Esc

Printer-friendly Version

Interactive Discussion



latitudes related to convective processes. An interesting feature pertains to changes along the Andes Mountains and Patagonia. During southern summer drier conditions during PD prevail over the southernmost regions. A sharp gradient is evident, separating the regions of wetter and drier conditions at approx. 50° S. An interesting point is that the drier conditions extend over the crest of the Andes Mountains into south-eastern Patagonia.

For southern summer the pattern is similar to winter, albeit with a shift of the wetter conditions during PD over southern South America to the north around 40° S. The sharp precipitation gradient is still evident in the region of Puerto Montt. In contrast to southern summer, south-eastern Patagonia is characterized by increased precipitation during PD compared to PI.

The annual mean precipitation pattern resembles to a large degree the average of the seasonal patterns. An important point is therefore the separate analysis of the different seasons to investigate changes in the seasonal precipitation cycle that would not be evident taking into account only annual mean changes (cf. also discussion in Wagner et al. (2007) for seasonal differences between the mid-Holocene and pre-industrial times).

The right panel of Fig. 6 shows changes in mean sea level pressure between the PD and PI period. The basic pattern shows a dipole structure for both winter and summer season, with PD pressure decreases south of 55° S and increases to the North of 50° S, mostly pronounced over the southwestern Atlantic Ocean. Also over the central Andes Mountains and the Altiplano pressure increases in the present-day climate. This pattern leads to an intensified westerly flow. Some regions showing an increase in sea level pressure, for example south-eastern Patagonia during southern summer, also show a decrease in precipitation during PD. This might be related to the suppression of convective processes. During southern winter the dipole pattern is shifted towards the North. Moreover, the pattern shows a more non-zonal component compared to southern summer, leading to a more northwesterly flow. The more northern position of the region with increased PD pressure conditions might explain the more widespread

Climate over South America in regional model simulations

S. Wagner et al.

Title Page

Abstract

Introduction

Conclusions

References

Tables

Figures



Back

Close

Full Screen / Esc

Printer-friendly Version

Interactive Discussion



the PI simulation for tropospheric levels at 200 hPa, 500 hPa and 850 hPa for southern summer and winter together with the annual mean. For comparison also changes in the ECHO-G simulation without CCLM are given. This is to assess whether the regional simulation shows differences compared to the driving GCM.

According to Table 2 largest changes in maximum zonal wind speed are evident during southern summer. This can especially be seen for the southward shift in the latitude of maximum wind speed. This southward shift is also accompanied by an increase in maximum wind speed, especially at the 850 hPa level. Differences between the RCM and GCM are also mostly pronounced at this level. This might be related to the stronger impact of the topography on near-surface winds in the RCM on the lower levels rather than the upper. Compared to southern summer, for southern winter only minor changes are evident. The regional model shows a slight southward shift in conjunction with a slight increase in maximum wind speed. Changes are however too small to attain statistical significance at the 5% level. The annual mean also shows a southward shift, mostly pronounced in the GCM. In the RCM a southward shift is evident at the 500 hPa and 850 hPa level, the latter showing also statistically significant increases in maximum winds.

To sum up, differences between present day and pre-industrial times in the context of changes in the latitude of zonal wind maximum mostly relate to a southward shift of the westerlies in conjunction with an increase in the maximum wind speed. Differences between the GCM and RCM with regard to latitudinal shifts are most likely due to the different grid spacing (0.44° in the RCM, 3.75° in the GCM), whereas changes in the mean maximum intensity are most likely due to the physical effects of the increased horizontal resolution, allowing for a better representation of the complex topography. Most important, however, is the fact that the basic pattern in changes in latitude and intensity of maximum of zonal wind component are similar in both simulations. This underpins the strong influence of the driving model in conditioning the dynamical situation of the RCM.

Climate over South America in regional model simulations

S. Wagner et al.

Title Page

Abstract

Introduction

Conclusions

References

Tables

Figures



Back

Close

Full Screen / Esc

Printer-friendly Version

Interactive Discussion



Climate over South America in regional model simulations

S. Wagner et al.

Title Page

Abstract

Introduction

Conclusions

References

Tables

Figures



Back

Close

Full Screen / Esc

Printer-friendly Version

Interactive Discussion



The analysis presented above addressed changes in the latitude and magnitude of the *maximum* of zonal wind. Spatially resolved changes of *mean* zonal wind at different tropospheric levels are displayed in Fig. 7. For southern summer a dipole pattern with increased zonal winds south of 45° S and reduced winds north of 40° S is evident for all levels. During southern winter a similar pattern is evident, albeit weaker in amplitude. Only at the 200 hPa level zonal winds show an increase in the northern parts of the domain. The annual mean patterns also show mainly a dipole pattern, mostly pronounced at the 850 hPa level. At this level more local-scale structures are evident, for example along the Andes Mountains. This phenomenon can be explained by the increased resolution of the topography within the RCM. Thus, changes in mean zonal wind patterns reveals that increases in wind speed in a specific latitude are accompanied by a reduction in wind speed in another latitudinal band. This pattern is mostly evident during southern summer, indicating that the summer season reacts most sensitive to changes in atmospheric greenhouse gas concentrations, also in terms of zonal winds. The spatial patterns contain valuable information in addition to solely analyzing changes in maximum wind speeds because also regions experiencing a reduction in zonal winds can be detected.

An interesting feature concerning changes in the wind patterns relates to the sign of change being similar for the southern summer and winter season, i.e. changes in maximum winds that point in the same direction in the different seasons. Results obtained for the comparison between the period of the mid-Holocene and pre-industrial times do however show a different pattern, indicating a more pronounced seasonal cycle in the latitude of maximum winds. This discrepancy might be explained by the different external forcing mechanisms primarily influencing the large-scale circulation in the different time periods. For the mid-Holocene, changes in orbital parameters can be used to explain changes in winds through changes in meridional temperature gradients and hence changes in the position of maximum baroclinicity (cf. Fig. 13 of Wagner et al., 2007). For the simulated differences between present-day and pre-industrial times only increase in greenhouse gas concentrations are responsible for changes in atmospheric

circulation. Greenhouse gas changes do not show any seasonal cycle and therefore the pattern of change between natural (i.e. orbital) and anthropogenic (i.e. greenhouse gases) might be reflected in changes in large-scale atmospheric circulation patterns in terms of changes of zonal winds.

5 Summary and conclusions

In the present study two simulations with the regional climate model CCLM have been investigated for climatic changes between present-day and pre-industrial times. The regional model was integrated on a $0.44^\circ \times 0.44^\circ$ grid resolution and was forced with global simulations of the ECHO-G model with a horizontal resolution of $3.75^\circ \times 3.75^\circ$.

The validation of the model against observation-based data sets shows in general that the model is able to capture the main climatological features, including the annual cycle. A point that should however be noted is that part of discrepancies between model and observations might also be due to the sparseness of observations complicating the comparison between modelling results. Moreover, especially differences in precipitation might be due to different bases of comparison with pointwise measurements for the observations and spatially aggregated means in the model. This issue becomes especially important for regions with complex terrain.

Some spatial model biases are however evident, for instance related to an overestimation of temperatures in the ECHO-G+CCLM simulation in large parts over eastern and central South America in conjunction with a negative precipitation bias in these regions. This bias is related to simulated SLP that is too high compared to observational data. In the southernmost parts a negative temperature bias in conjunction with positive precipitation biases is simulated by the present-day ECHO-G+CCLM simulation. These biases can in turn be explained by sea level pressure biases over these areas that are too low, leading to an increased westerly flow.

Climate changes between present-day and pre-industrial times show a quite uniform pattern for near-surface temperatures with an increase over most areas, mostly

Climate over South America in regional model simulations

S. Wagner et al.

Title Page

Abstract

Introduction

Conclusions

References

Tables

Figures



Back

Close

Full Screen / Esc

Printer-friendly Version

Interactive Discussion



Climate over South America in regional model simulations

S. Wagner et al.

Title Page

Abstract

Introduction

Conclusions

References

Tables

Figures



Back

Close

Full Screen / Esc

Printer-friendly Version

Interactive Discussion



pronounced over the Andes Mountains. This change is due to the increased greenhouse gas concentrations. Precipitation changes show a spatially more complex pattern. For example, increases and decreases of precipitation are evident along the western side of the Andes Mountains. These changes can be linked to changes in the strength of westerly winds. An important feature, also in the context of paleoclimatic reconstructions relates to the change of sign from positive to negative values within 10th of kilometers. This should be taken into account when interpreting proxy data located within the regions of strong hydrological gradients.

A notable finding in this respect relates to the fact that despite the quite homogenous pattern for the temperature changes, differences related to hydrological variables show a much more complex pattern. This applies not only to the very complex spatial pattern of change but also to changes between the different seasons. This point is of specific interest for reconstructing climate indices based on empirical evidence. Results based on the regional climate simulations suggest that it is of ultimate importance to establish transfer functions based on seasonal rather than annual averages. As shown for the hydrological variables, changes between seasons could not only be different in magnitude but also different in terms of sign. Taking this result into account could potentially be used to revisit some of the already established hypothesis related to changes in hydrological climate in South America and changes in westerly winds.

Changes in westerly winds between present-day and pre-industrial times show a general increase in the maximum zonal wind velocity and a southward shift. This movement is mostly pronounced during southern summer. The spatial differences display a dipole pattern with increased wind speeds at all tropospheric levels over the extratropical parts south of 45° S and wind speed decreases north of 40° S. The pattern is also very similar in all seasons, with the exception of the 200 hPa level during southern summer showing primarily increased wind speeds.

Results presented here for the present-day minus pre-industrial changes show interesting links to an earlier study carried out for the mid-Holocene by Wagner et al. (2007). During the mid-Holocene an increase in the seasonal amplitude in changes in westerly

Climate over South America in regional model simulations

S. Wagner et al.

Title Page

Abstract

Introduction

Conclusions

References

Tables

Figures

⏪

⏩

◀

▶

Back

Close

Full Screen / Esc

Printer-friendly Version

Interactive Discussion



winds is evident, whereas changes in wind between the PD and PI period show the same pattern for all seasons. The reason explaining this phenomenon might relate to different external forcing mechanisms: For the mid-Holocene changes in orbital forcing, exerting a pronounced influence on the seasonal distribution of incoming solar radiation, produce also a seasonal amplified change of the atmospheric circulation. Changes in forcings between the PD and PI period, namely increase of greenhouse gases, exert a similar influence on the atmospheric circulation over the entire year in terms of a shift of the westerly winds, resulting in the dipole pattern described above. The driving mechanisms have not been explored in detail here but it could be expected that similar processes are responsible for this shift in terms of changes in meridional temperature gradients due to increased greenhouse gas concentrations.

The added value using a regional climate model instead of the raw GCM output also relates to a better representation of near-surface winds, for example at the 850 hPa level. Here the increased horizontal and vertical resolution of the RCM allows for a better simulation of winds that are influenced by mountain ranges, i.e. the Andes Mountains. However, the overall sign of change in terms of maximum winds and the corresponding latitudes are similar, pointing to the prominent influence of the driving GCM on the atmospheric circulation in the RCM, especially in the middle and upper troposphere.

The main conclusions of the study can thus be summarized as follows:

1. The regional climate model CCLM is able to capture the mean climatological features related to temperature and precipitation for the climatological (here 5 yr) mean and the annual cycle.
2. Near-surface temperatures between present-day and pre-industrial times show positive temperature anomalies over most regions over southern and central South America in the order of 1–1.5 K, and up to 2 K over the Andes Mountains.
3. Precipitation differences show a more heterogeneous pattern with highest differences along the western side of the Andes Mountains in conjunction with a dipole

pattern indicating reduced precipitation in the northern parts and increased precipitation in the southern parts of southern South America during PD.

4. Changes in westerly winds are in accordance with the driving GCM, especially for the middle and upper troposphere. In the lower levels differences in the westerlies are evident that can be explained by the influence of the topography which is better represented in the RCM.

These latitudinal and intensity changes in westerly winds can also explain changes in precipitation. In contrast, temperature changes are primarily driven by the increased greenhouse gas concentrations and the direct thermodynamic feedback.

The modelled temperature changes presented in this study in the order of 1–2 K between present-day and pre-industrial times overestimate the reconstructed ones by Neukom et al. (2010a) and Villalba et al. (2003) by approximately a factor of two. The reconstruction of Neukom et al. (2010a) for summer temperatures for different southern South American regions shows similar levels in the late 20th century and the late 18th century, whereas in the 15th and 16th century temperatures were considerably lower compared to present-day (approx. 2 K for southern Patagonia). Winter temperatures show highest levels at the beginning of the 20th century followed by a slight decline (Fig. 6 of Neukom et al., 2010a). Lowest temperatures are reconstructed however for the 18th century around 1750 AD. In general, temperature differences between the 20th century and earlier centuries are more pronounced the more southward the region is located. The latter phenomenon is not evident in the regional climate model simulations.

Precipitation changes simulated by the model and reconstructed by Neukom et al. (2010b) deviate quite profoundly concerning the spatial extent and sign of positive and negative precipitation changes between the 20th century and the former centuries. The only region with similar changes in the model and the reconstruction can be located over southern Patagonia during southern summer. The strong decrease in reconstructed precipitation over entire southern South America during southern winter

Climate over South America in regional model simulations

S. Wagner et al.

Title Page

Abstract

Introduction

Conclusions

References

Tables

Figures



Back

Close

Full Screen / Esc

Printer-friendly Version

Interactive Discussion



is not reflected in the simulations. Instead, the model shows a dipole pattern with reduced precipitation in the northern and increased precipitation in the southern parts. Reasons that might explain the discrepancies between model and reconstruction might be related to (i) different periods used in the reconstruction and modelling (the late 20th century and 1750s for the model and most of the 20th century compared to the former centuries in the reconstruction), (ii) the complex nature of processes controlling precipitation changes and (iii) uncertainties involved in both, the reconstruction and the downscaling model chain.

Changes in westerly winds and their effect on precipitation changes are also evident in the RCM simulation and therefore confirm their importance already outlined in other modelling studies (cf. Wyrwoll et al., 2000; Wagner et al., 2007; Garreaud et al., 2009; Rojas et al., 2009). The RCM simulation shows however improvements at lower tropospheric levels owing to the better representation of orographic features. A point that could not explicitly be accounted for in the RCM simulations is the onset and impact of human occupation that is presumably important on the local scale (cf. Mayr et al., 2005; Ariztegui et al., 2010) and potentially also affects hydrological changes, especially in the more arid- and semi-arid parts east to the Andes Mountains.

6 Outlook

The output of the regional climate model simulations can also be used to drive forward models, allowing for the direct modelling of proxy data. For some forward models the horizontal resolution of the regional climate model in the order of 10th of kilometres is however still too coarse. A possibility to overcome this problem is to carry out nested climate simulations with considerably increased resolution up to 1 km. Even though this does not eliminate the influence of the driving GCM it will however allow a more realistic representation of other small-scale processes, for example related to open convection, as well as pedological and vegetational characteristics.

Climate over South America in regional model simulations

S. Wagner et al.

Title Page

Abstract

Introduction

Conclusions

References

Tables

Figures



Back

Close

Full Screen / Esc

Printer-friendly Version

Interactive Discussion



Climate over South America in regional model simulations

S. Wagner et al.

Title Page

Abstract

Introduction

Conclusions

References

Tables

Figures

⏪

⏩

◀

▶

Back

Close

Full Screen / Esc

Printer-friendly Version

Interactive Discussion



Another important point that needs to be addressed is the implementation of (i) ensemble RCM simulations and (ii) the use of different GCMs as for instance used in the PMIP II project. In the context of proxy-model comparison this will enable the establishment of confidence intervals for different regional to local climatic states under the same external forcing conditions but with different GCMs and/or oceanic boundary conditions.

In the present study results of only one RCM have been discussed. As for the GCMs it could also be expected for the RCMs to show different responses even when the same GCM forcing is applied. This might for instance be caused by different convection schemes or different soil models employed in the respective RCM. Even though points outlined above seem to be demanding they should at least be addressed to assess the bandwidth of natural and anthropogenically forced climatic variability from a modelling perspective.

Acknowledgements. The simulations have been carried out in the framework of the project “Regional climate modelling in southern South America for the Holocene and the 21st century – REGCLIMOSS” funded by the German Research foundation. The regional climate model simulations have been carried out on a NEC-SX6 at the German Climate Computing Center.



The publication of this article was sponsored by PAGES.

References

- Ariztegui, D., Gilli, A., Anselmetti, F. S., Goni, R. A., Belardi, J. B., and Espinosa, S.: Lake-level changes in central Patagonia (Argentina): crossing environmental thresholds for Lateglacial and Holocene human occupation, *J. Quaternary Sci.*, 25, 1092–1099, 2010.
- Böhm, U., Gerstengarbe, F.-W., Hauffe, D., Kücken, M., Österle, H., and Werner, P. C.: Dynamic regional climate modeling and sensitivity experiments for the northeast of Brazil, in: *Global Change and Regional Impacts*, edited by: Gaiser, T., Krol, M., Frischkorn, H., and Araújo, J. C., Springer-Verlag Berlin Heidelberg New York, 153–170, 2003.

Climate over South America in regional model simulations

S. Wagner et al.

Title Page

Abstract

Introduction

Conclusions

References

Tables

Figures

◀

▶

◀

▶

Back

Close

Full Screen / Esc

Printer-friendly Version

Interactive Discussion



- Braconnot, P., Otto-Bliesner, B., Harrison, S., Joussaume, S., Peterchmitt, J.-Y., Abe-Ouchi, A., Crucifix, M., Driesschaert, E., Fichet, Th., Hewitt, C. D., Kageyama, M., Kitoh, A., Laine, A., Loutre, M.-F., Marti, O., Merkel, U., Ramstein, G., Valdes, P., Weber, S. L., Yu, Y., and Zhao, Y.: Results of PMIP2 coupled simulations of the Mid-Holocene and Last Glacial Maximum - Part 1: experiments and large-scale features, *Clim. Past*, 3, 261–277, doi:10.5194/cp-3-261-2007, 2007.
- Frei, C., Schöll, R., Fukutome, S., Schmidli, J., and Vidale, P. L.: Future change of precipitation extremes in Europe: Intercomparison of scenarios from regional climate models, *J. Geophys. Res.*, 111, D06105, 2006.
- Garreaud, R. D.: Cold air incursions over subtropical South America: Mean structure and dynamics, *Mon. Weather Rev.*, 128, 2544–2559, 2000.
- Garreaud, R. D., Vuille, M., Compagnucci, R., and Marengo, J.: Present day South American climate, *Palaeogeogr. Palaeoecol.*, 281, 180–195, 2000.
- Gómez-Navarro, J. J., Montávez, J. P., Jerez, S., Jiménez-Guerrero, P., Lorente-Plazas, R., González-Rouco, J. F., and Zorita, E.: A regional climate simulation over the Iberian Peninsula for the last millennium, *Clim. Past*, 7, 451–472, doi:10.5194/cp-7-451-2011, 2011.
- Haberzettl, T., Fey, M., Lücke, A., Maidana, N., Mayr, C., Ohlendorf, C., Schäbitz, F., Schleser, G. H., Wille, M., and Zolitschka, B.: Climatically induced lake level changes during the last two millennia as reconstructed in sediments of Laguna Potrok Aike, southern Patagonia (Santa Cruz, Argentina), *J. Paleolimnol.*, 33, 283–302, 2005.
- Insel, N., Poulsen, C. J., and Ehlers, T. A.: Influence of the Andes Mountains on South American Moisture Transport, Convection, and Precipitation, *Clim. Dynam.*, 35, 1477–1492, 2009.
- Kistler, R., Kalnay, E., Collins, W., Saha, S., White, G., Woollen, J., Chelliah, M., Ebisuzaki, W., Kanamitsu, M., Kousky, V., van den Dool, H., Jenne, R., and Fiorino, M.: The NCEP/NCAR 50-year reanalysis: monthly means CD ROM and documentation, *B. Am. Meteorol. Soc.*, 82, 47–267, 2001.
- Lamy, F., Hebbeln, D., Röhl, U., and Wefer, G.: Holocene rainfall variability in southern Chile: a marine record of latitudinal shifts of the Southern Westerlies, *Earth Planet. Sc. Lett.*, 185, 369–382, 2001.
- Lamy, F., Kilian, R., Arz, H. W., Francois, J. P., Kaiser, J., Prange, M., and Steinke, T.: Holocene changes in the position and intensity of the southern westerly wind belt, *Nat. Geosci.*, 3, 695–699, 2010.
- Legutke, S. and Voss, R.: The Hamburg atmosphere-ocean coupled model ECHO - G, Tech.

Climate over South America in regional model simulations

S. Wagner et al.

Title Page

Abstract

Introduction

Conclusions

References

Tables

Figures

◀

▶

◀

▶

Back

Close

Full Screen / Esc

Printer-friendly Version

Interactive Discussion



Rep., 18, German Climate Computer Center (DKRZ), available at: www.mad.zmaw.de/fileadmin/extern/documents/reports/ReportNo.18.pdf, 1999.

Markgraf, V., Bradbury, J., Schwalb, A., Burns, S., Stern, C., Ariztegui, D., Anselmetti, F., Stine, S., and Maidana, N.: Holocene palaeoclimates of southern Patagonia: limnological and environmental history of Lago Cardiel, Argentina, *Holocene*, 13, 581–591, 2003.

Mayr, C., Fey, M., Habertzettl, T., Janssen, S., Lücke, A., Maidana, N., Ohlendorf, C., Schäbitz, F., Schleser, G., Struck, U., Wille, M., and Zolitschka, B.: Palaeoenvironmental changes in southern Patagonia during the last millennium recorded in lake sediments from Laguna Azul (Argentina), *Palaeogeogr. Palaeoecol.*, 228, 203–227, 2005.

Meehl, G. A., Boer, G. J., Covey, C., Latif, M., and Stouffer, R. J.: The Coupled Model Inter-comparison Project (CMIP), *B. Am. Meteorol. Soc.*, 81, 313–318, 2000.

Mitchell, T. D. and Jones, P. D.: An improved method of constructing a database of monthly climate observations and associated high-resolution grids, *Int. J. Climatol.*, 25, 693–712, 2005.

Moreno, P., François, J. P., Villa-Martínez, R. P., and Moy, C. M.: Millennial-scale variability in Southern Hemisphere westerly wind activity over the last 5,000 years in SW Patagonia, *Quaternary Sci. Rev.*, 28, 25–38, 2009.

Moy, C. M., Dunbar, R. B., Moreno, P. I., Francois, J. P., Villa-Martinez, R., Mucciarone, D. A., Guilderson, T. P., and Garreaud, R. D.: Isotopic Evidence for Hydrologic Change Related to the Westerlies in SW Patagonia, Chile During the Last Millennium, *Quaternary Sci. Rev.*, 27, 1335–1349, 2008.

Neukom, R., Luterbacher, J., Villalba, R., Küttel, M., Frank, D., Jones, P. D., Grosjean, M., Wanner, H., Aravena, J. C., Black, D. E., Christie, D. A., D'Arrigo, R., Lara, A., Morales, M., Soliz-Gamboa, C., Srur, A., Urrutia, R., and von Gunten, L.: Multiproxy summer and winter surface air temperature field reconstructions for southern South America covering the past centuries, *Clim. Dynam.*, 37, 35–51, 2010a.

Neukom, R., Luterbacher, J., Villalba, R., Küttel, M., Frank, D., Jones, P. D., Grosjean, M., Esper, J., Lopez, L., and Wanner, H.: Multi-centennial summer and winter precipitation variability in southern South America, *Geophys. Res. Lett.*, 37, L14708, doi:10.1029/2010GL043680, 2010b.

Melo, M. L. D. and Marengo, J. A.: The influence of changes in orbital parameters over South American climate using the CPTEC AGCM: Simulation of climate during the mid Holocene, *Holocene*, 18, 501–516, 2008.

Climate over South America in regional model simulations

S. Wagner et al.

Title Page

Abstract

Introduction

Conclusions

References

Tables

Figures



Back

Close

Full Screen / Esc

Printer-friendly Version

Interactive Discussion



- Min, S.-K., Legutke, S., Hense, A., and Kwon, W.-T.: Internal variability in a 1000-year control simulation with the coupled climate model ECHO-G – I. Near-surface temperature, precipitation and mean sea level pressure, *Tellus*, 57A, 605–621, 2005.
- Misra, V., Dirmeyer, P. A., and Kirtman, B. P.: Dynamic Downscaling of Seasonal Simulations over South America, *J. Climate*, 16, 103–117, 2003.
- Núñez, M. N., Solman, S. A., and Cabré, M. F.: Regional climate change experiments over southern South America. II: Climate change scenarios in the late twenty-first century, *Clim. Dynam.*, 32, 1081–1095, 2008.
- PMIP, Paleoclimate Modeling Intercomparison Project (PMIP): proceedings of the third PMIP workshop, Canada, 4–8 October 1999, in: WCRP-111, WMO/TD-1007, edited by: Braconnot, P., 271 pp., 2000.
- Poulsen, C. J., Ehlers, T. A., and Insel, N.: Onset of convective rainfall during gradual Late Miocene rise of the Central Andes, *Science*, 328, 490–493, 2010.
- Rockel, B. and Geyer, B.: The performance of the regional climate model CLM in different climate regions, based on the example of precipitation, *Meteorol. Z.*, 17, 487–498, 2008.
- Roeckner, E., Arpe, K., Bengtsson, L., Christoph, M., Claussen, M., Dümenil, L., Esch, M., Giorgetta, M., Schlese, U., and Schulzweida, U.: The atmospheric general circulation model ECHAM4: model description and simulation of present-day climate, *Tech. Rep.*, 218, Max Planck Institut für Meteorologie, 1996.
- Rojas, M., Moreno, P., Kageyama, M., Crucifix, M., Hewitt, C., Abe-Ouchi, A., Ohgaito, R. C., Brady, E. C., and Hope, P.: The Southern Westerlies during the last glacial maximum in PMIP2 simulations, *Clim. Dynam.*, 32, 525–548, 2009.
- Rudolf, B., Becker, A., Schneider, U., Meyer-Christoffer, A., Ziese, M.: GPCP Status Report, Global Precipitation Climatology Center, available at: <http://gpcc.dwd.de>, 2010.
- Salio, P., Nicolini, M., and Saulo, A. C.: Chaco low-level jet events characterization during the austral summer season, *J. Geophys. Res.*, 107, 4816, doi:T0.1029/2001JD001315, 2002.
- Schäbitz, F.: Paläoökologische Untersuchungen an geschlossenen Hohlformen in den Trockengebieten Patagoniens, *Tech. Rep.*, 17, Universität Bamberg, 1999.
- Seluchi, M. E., Garreaud, R. D., Norte, F. A., and Saulo, A. C.: Influence of the Subtropical Andes on Baroclinic Disturbances: A Cold Front Case Study, *Mon. Weather Rev.*, 134, 3317–3335, 2006.
- Seth, A. and Rojas, M.: Simulation and Sensitivity in a Nested Modeling System for South America. Part I: Reanalyses Boundary Forcing, *J. Climate*, 16, 2437–2453, 2003.

Climate over South America in regional model simulations

S. Wagner et al.

Title Page

Abstract

Introduction

Conclusions

References

Tables

Figures

◀

▶

◀

▶

Back

Close

Full Screen / Esc

Printer-friendly Version

Interactive Discussion



- Silvestri, E. and Vera, C.: Antarctic Oscillation signal on precipitation anomalies over south-eastern South America, *Geophys. Res. Lett.*, 30, 2115, doi:10.1029/2003GL018277, 2003.
- Silvestri, G., Vera, C., Jacob, D., Pfeifer, S., and Teichmann, C.: A high resolution 43-year atmospheric hindcast for South America generated with the MPI regional model, *Clim. Dynam.*, 32, 693–709, 2009.
- Solman, S., Nuñez, M., and Cabré, M. F.: Regional climate change experiments over southern South America. I: present climate, *Clim. Dynam.*, 30, 533–552, 2008.
- Varma, V., Prange, M., Lamy, F., Merkel, U., and Schulz, M.: Solar-forced shifts of the Southern Hemisphere Westerlies during the Holocene, *Clim. Past*, 7, 339–347, doi:10.5194/cp-7-339-2011, 2011.
- Vera, C., Silvestri, G., Liebmann, B., and González, P.: Climate change scenarios for seasonal precipitation in South America from IPCC-AR4 models, *Geophys. Res. Lett.*, 33, L13707, doi:10.1029/2006GL025759, 2006.
- Villa-Martínez, R. and Moreno, P. I.: Pollen evidence for variations in the southern margin of the westerly winds in SW Patagonia over the last 12,600 years, *Quaternary Res.*, 68, 400–409, 2007.
- Villalba, R., Lara, A., Boninsegna, J. A., Masiokas, M., Delgado, S., Aravena, J. C., Roig, F. A., Schmelter, A., Wolodarsky, A., and Ripalta, A.: Large-scale temperature changes across the southern Andes: 20th-century variations in the context of the past 400 years, *Climatic Change*, 177–232, 2003.
- Wagner, S., Widmann, M., Jones, J., Haberzettl, T., Lücke, A., Mayr, C., Ohlendorf, C., Schäbitz, F., and Zolitschka, B.: Transient simulations, empirical reconstructions and forcing mechanisms for the Mid-Holocene hydrological climate in Southern Patagonia, *Clim. Dynam.*, 29, 333–355, 2007.
- Wiedenmann, J. M., Lupo, A. R., Mokhov, I. I., and Tikhonova, E. A.: The Climatology of Blocking Anticyclones for the Northern and Southern Hemispheres: Block Intensity as a Diagnostic, *J. Climate*, 15, 3459–3473, 2002.
- Wolff, J., Maier-Reimer, E., and Legutke, S.: The Hamburg Primitive Equation Model HOPE, *Tech. Rep.*, 18, German Climate Computer Center (DKRZ), 1997.
- Wyrwoll, K., Dong, B., and Valdes, P.: On the position of southern hemisphere westerlies at the Last Glacial Maximum: an outline of AGCM simulation results and evaluation of their implications, *Quaternary Sci. Rev.*, 19, 881–398, 2000.

Climate over South America in regional model simulations

S. Wagner et al.

Table 1. Climate stations representing selected climatic regions (modified after Solman et al., 2008).

Acronym	Region	Station	lat	lon
CA	Central Andes	Antofagasta	23.5° S	70.5° W
SUA	Subtropical Andes	Santiago de Chile	33.5° S	70.5° W
LPB	La Plata Basin	Santa Fe	31.5° S	60.5° W
SB	Southern Brazil	Porto Alegre	30° S	51° W
SA	Southern Andes	Puerto Montt	41.5° S	73° W
AP	Argentinean Patagonia	Rio Gallegos	51.5° S	69° W

Title Page

Abstract

Introduction

Conclusions

References

Tables

Figures

◀

▶

◀

▶

Back

Close

Full Screen / Esc

Printer-friendly Version

Interactive Discussion



Climate over South America in regional model simulations

S. Wagner et al.

Table 2. Mean position ($^{\circ}$ S) [and *intensity* (m s^{-1})] of maximum zonal winds along 70° W for the pre-industrial (PI) and present-day (PD) simulation. The columns under ECHO-G display results for ECHO-G alone, the columns under ECHO-G+CCLM show results for the regional climate model simulation forced with ECHO-G. The difference to the pre-industrial simulation is given in parentheses. For the position, “–” indicates a more equatorward, “+” indicates a more poleward position during present-day period. The asterisk indicates values significantly different at the 5 % level (two-sided test). DJF: December–February, JJA: June–August, ANN = annual mean.

	ECHO-G		ECHO-G+CCLM	
	PI	PD	PI	PD
DJF				
U200	42.0 [36.9]	45.2 (+3.2*) [36.5 (–0.4)]	40.9 [36.8]	43.7 (+2.8*) [36.4 (–0.4)]
U500	44.2 [19.9]	47.5 (+3.3*) [20.6 (+0.7*)]	43.0 [20.2]	45.9 (+2.9*) [20.2 (\pm 0)]
U850	49.3 [11.8]	51.6 (+2.3*) [13.3 (+1.5*)]	46.4 [13.7]	49.6 (+3.2*) [14.6 (+0.9*)]
JJA				
U200	30.2 [42.1]	31.2 (+1.0) [44.0 (+1.9*)]	28.6 [41.5]	28.7 (+0.1) [43.2 (+1.7)]
U500	39.0 [21.2]	38.1 (–0.9) [21.6 (+0.4)]	35.7 [23.9]	36.3 (+0.6) [24.0 (+0.1)]
U850	45.6 [11.0]	46.4 (+0.8) [11.3 (+0.3)]	42.1 [15.0]	43.3 (+1.2) [15.6 (+0.6)]
ANN				
U200	38.7 [34.7]	38.3 (–0.4) [35.4 (+0.7)]	38.7 [34.2]	38.2 (–0.5) [34.6 (+0.2)]
U500	41.8 [18.3]	44.3 (+2.5*) [18.6 (+0.3)]	40.4 [19.3]	42.6 (+2.2*) [19.4 (+0.1)]
U850	47.3 [10.0]	50.0 (+2.7*) [11.2 (+1.2*)]	44.6 [12.9]	45.7 (+1.1*) [13.5 (+0.6*)]

[Title Page](#)
[Abstract](#)
[Introduction](#)
[Conclusions](#)
[References](#)
[Tables](#)
[Figures](#)
[Back](#)
[Close](#)
[Full Screen / Esc](#)
[Printer-friendly Version](#)
[Interactive Discussion](#)


Climate over South America in regional model simulations

S. Wagner et al.

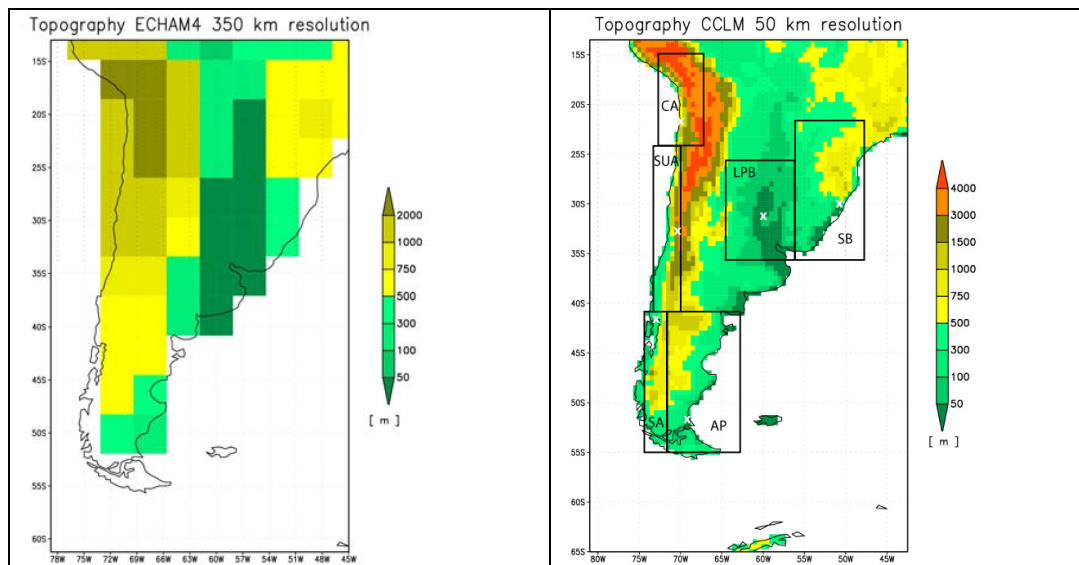


Fig. 1. Comparison between the topography of the global model ECHO-G (350 km) and the regional model CCLM (50 km). In the right panel regions for comparisons with observations are indicated (cf. Solman et al., 2008). The white crosses indicate the locations representative of the specific region (cf. Table 1).

[Title Page](#)[Abstract](#)[Introduction](#)[Conclusions](#)[References](#)[Tables](#)[Figures](#)[◀](#)[▶](#)[◀](#)[▶](#)[Back](#)[Close](#)[Full Screen / Esc](#)[Printer-friendly Version](#)[Interactive Discussion](#)

Climate over South America in regional model simulations

S. Wagner et al.

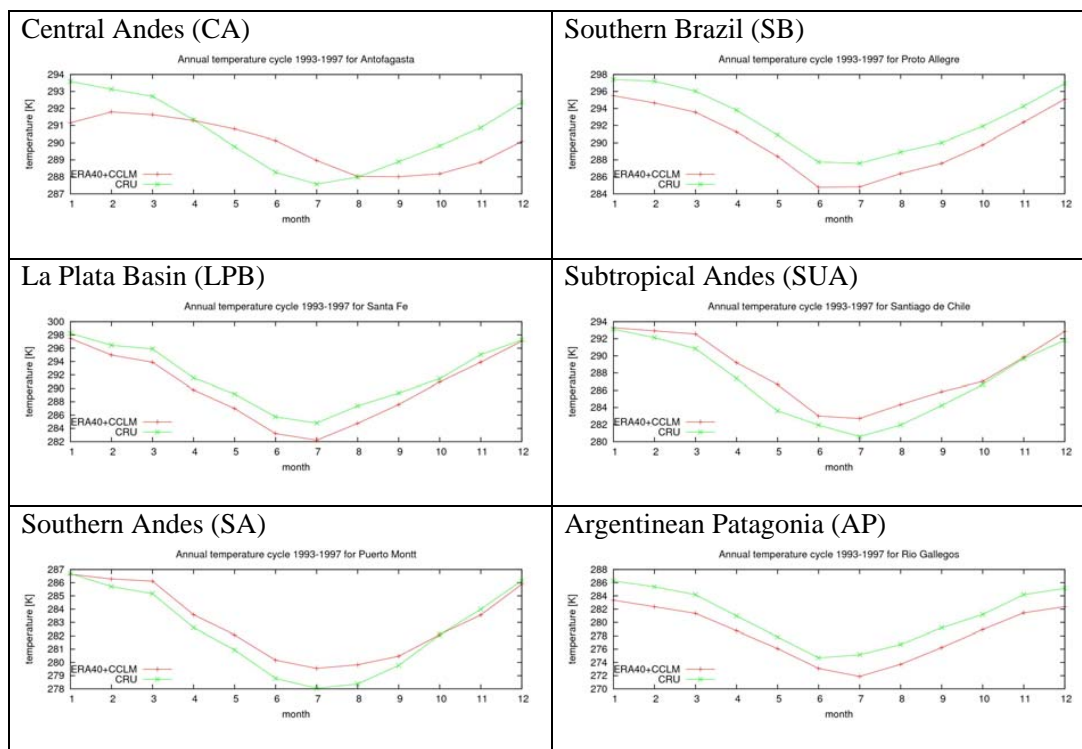


Fig. 2a. Model validation for the annual temperature cycle for the period 1993–1997 for grid points co-located with locations where observational data are available for ERA40+CCLM (red line) and CRU (green line). Geographical locations are provided in Table 1 together with regions defined by Solman et al. (2008).

Title Page

Abstract

Introduction

Conclusions

References

Tables

Figures

◀

▶

◀

▶

Back

Close

Full Screen / Esc

Printer-friendly Version

Interactive Discussion



Climate over South America in regional model simulations

S. Wagner et al.

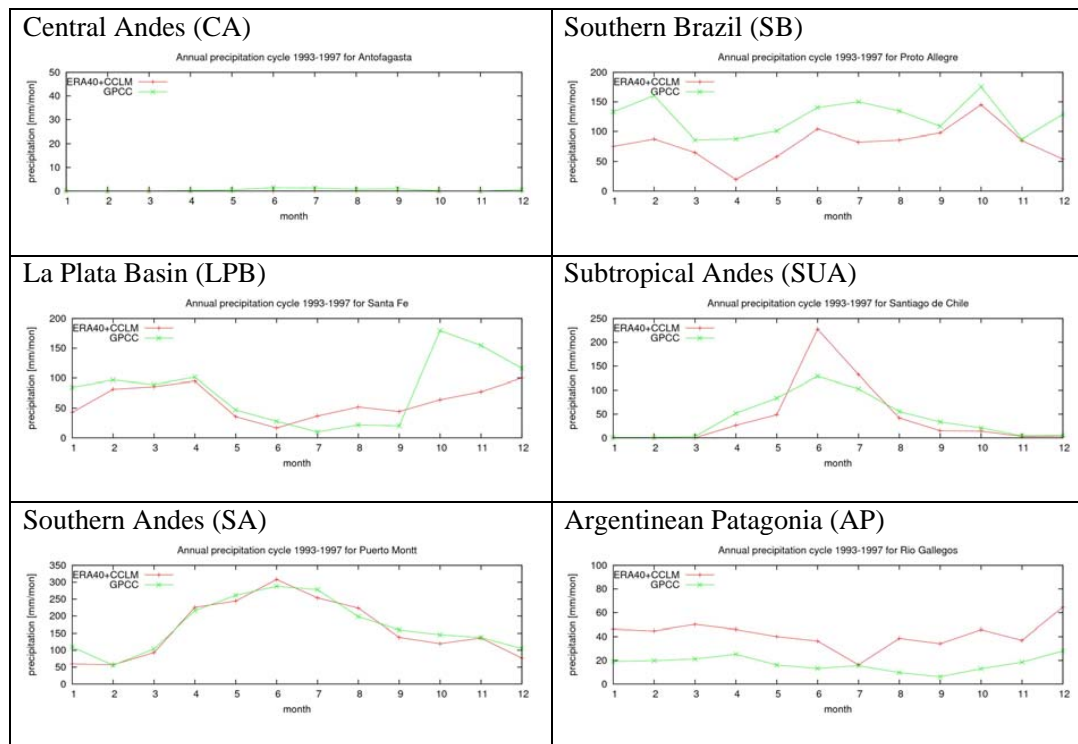


Fig. 2b. Same as Fig. 2a except for the annual precipitation cycle. The red line shows the annual cycle for the ERA40+CCLM simulation, the green line the one for the GPCCC data set.

Title Page

Abstract

Introduction

Conclusions

References

Tables

Figures

◀

▶

◀

▶

Back

Close

Full Screen / Esc

Printer-friendly Version

Interactive Discussion



Climate over South America in regional model simulations

S. Wagner et al.

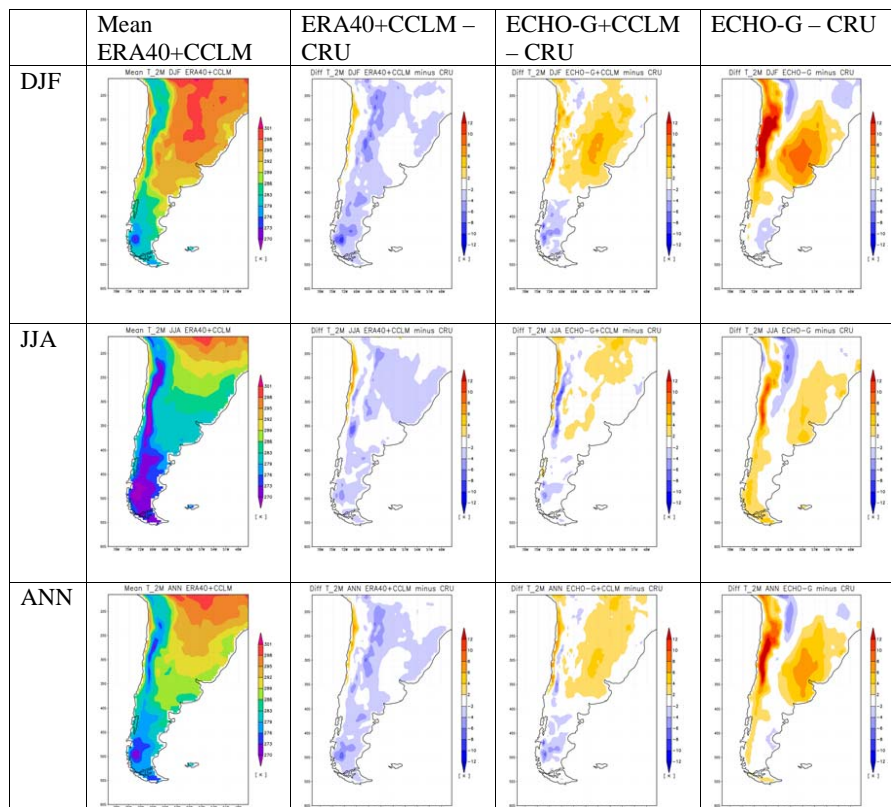


Fig. 3. Temperature fields for the different simulations. The left column shows the mean of the ERA40+CCLM simulation for December–February (DJF, upper), June–August (middle) and the annual average (lower) for the period 1993–1997. The second column shows the differences to the CRU data set for the same period. The 3rd and 4th columns show the differences of the ECHO-G+CCLM simulation and the ECHO-G simulation for present-day, respectively.

Title Page

Abstract

Introduction

Conclusions

References

Tables

Figures

◀

▶

◀

▶

Back

Close

Full Screen / Esc

Printer-friendly Version

Interactive Discussion



Climate over South America in regional model simulations

S. Wagner et al.

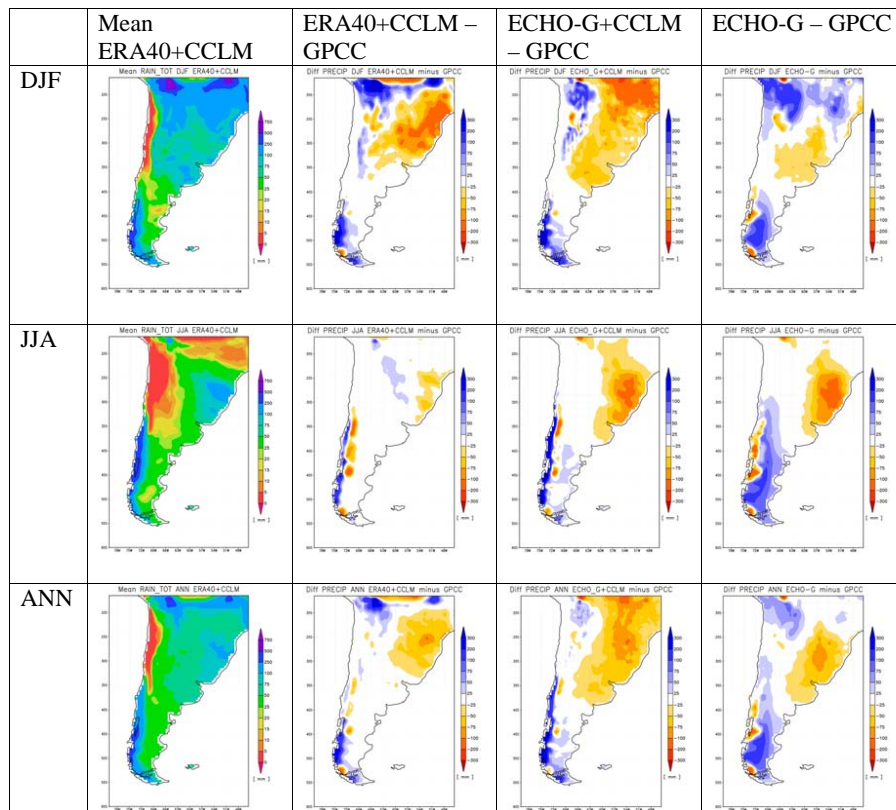


Fig. 4. Same as Fig. 3 except for precipitation based on the GPCC data set.

Title Page

Abstract

Introduction

Conclusions

References

Tables

Figures

◀

▶

◀

▶

Back

Close

Full Screen / Esc

Printer-friendly Version

Interactive Discussion



Climate over South America in regional model simulations

S. Wagner et al.

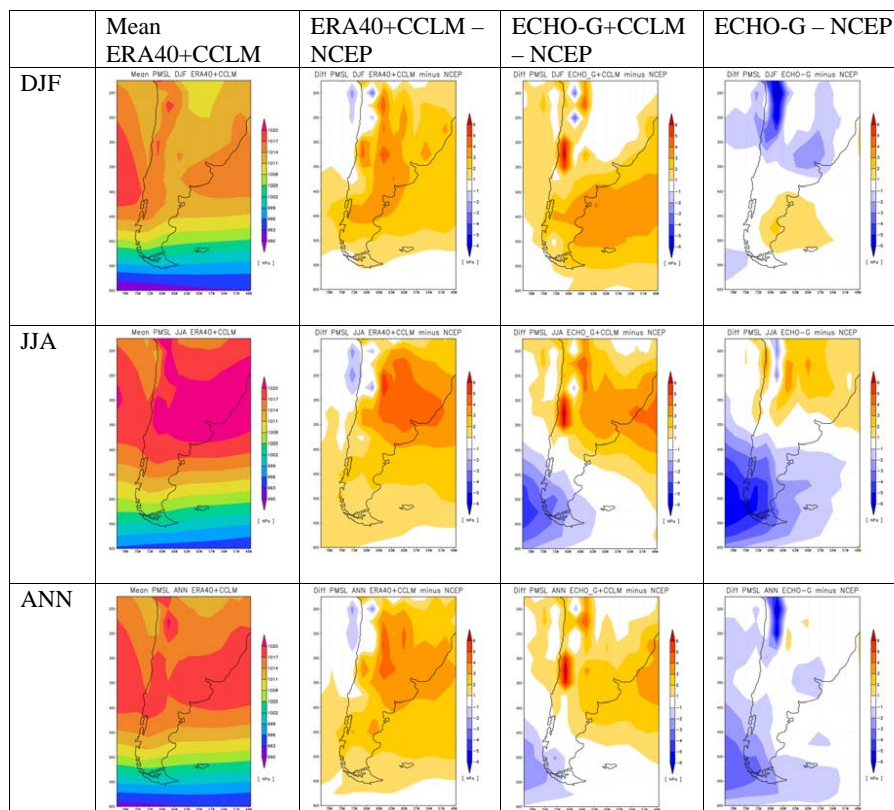


Fig. 5. Same as Fig. 3 except for sea level pressure. As reference the NCEP/NCAR data set has been used.

Title Page

Abstract

Introduction

Conclusions

References

Tables

Figures



Back

Close

Full Screen / Esc

Printer-friendly Version

Interactive Discussion



Climate over South America in regional model simulations

S. Wagner et al.

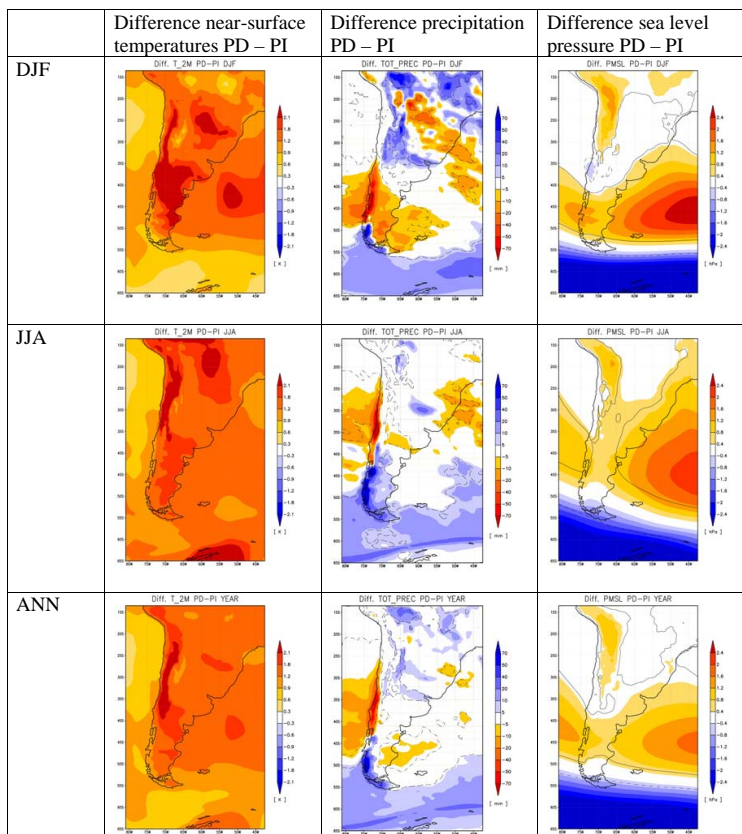


Fig. 6. Difference maps between the present-day and the pre-industrial periods for near-surface temperature (left column), precipitation (middle column) and sea level pressure (right column). Results are displayed for southern summer (December–February, upper row), southern winter (June–August, middle row) and the annual mean (lower row).

Title Page

Abstract

Introduction

Conclusions

References

Tables

Figures

◀

▶

◀

▶

Back

Close

Full Screen / Esc

Printer-friendly Version

Interactive Discussion



Climate over South America in regional model simulations

S. Wagner et al.

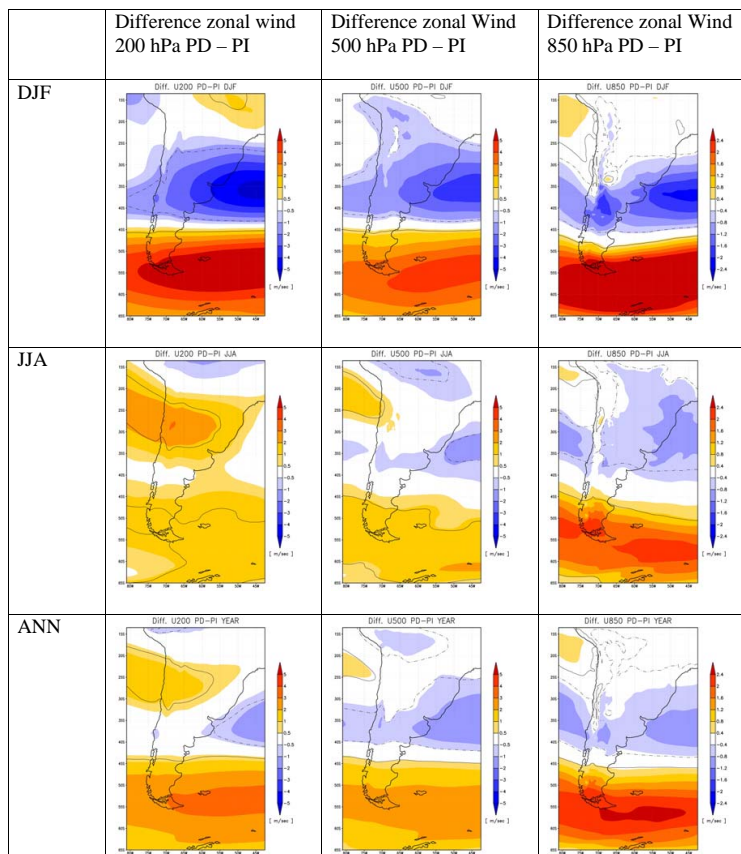


Fig. 7. Difference maps between the present-day and the pre-industrial period for zonal winds for different atmospheric levels at 200 hPa (left row), 500 hPa (middle panel) and 850 hPa (right row). Results are displayed for southern summer (December–February, left column), southern winter (June–August, middle column) and the annual mean (right column).

Title Page

Abstract

Introduction

Conclusions

References

Tables

Figures

◀

▶

◀

▶

Back

Close

Full Screen / Esc

Printer-friendly Version

Interactive Discussion

